

Effects of thermal and mechanical cyclic loads on polyurethane pre-insulated pipes

Lucía Doyle  | Ingo Weidlich 

Department of Infrastructural Engineering, HafenCity University, Hamburg, Germany

Correspondence

Lucía Doyle, Department of Infrastructural Engineering, HafenCity University, Überseeallee 16, Hamburg, Germany.
Email: lucia.doyle@hcu-hamburg.de

Funding information

HafenCity University

Abstract

District heating (DH) pre-insulated pipes are a sandwich assembly composed by a steel heat service pipe, polyurethane (PU) foam and polyethylene casing. The foam acts as bond between the steel pipe and casing. The application has high constraints for the foam, as it is subjected to cyclic multiaxial stresses, high cyclic temperatures and long expected service life. In this study, we evaluate if and how cyclic loads affect the shear strength, shear modulus, toughness and failure behaviour of the PU foam in DH pipes sandwich assembly compared with unaged reference samples. We have found that the simultaneous application of mechanical and thermal loads weakens the strength and increases the stiffness of the foam and that this change is not caused by degradation of the molecular structure. Crack initiation and propagation along the pipe samples follow a very consistent pattern between samples, with cracks initiating in Mode II and propagating in Mode I. The consistent axial displacement of approximately 2 cm from each other suggests the formation of strain localizations.

KEYWORDS

cyclic loading, district heating, fatigue, foam, polyurethane, sandwich structure

1 | INTRODUCTION

District heating (DH) pre-insulated pipes sandwich assembly composed of a steel heat service pipe, insulating material (polyurethane [PU] foam) and polyethylene (PE) casing, which are bonded by the insulating material.¹ The pipe networks are directly buried underground. The DH system's start-up and shut downs, as well as fluctuations on heat demand and ambient temperature, subject the piping network to thermal and mechanical cycling due to the thermal expansion. The axial expansion of the pipes is partially counteracted by frictional forces acting between the ground and the casing, with

the shear stresses transferred through the PU foam bond. Therefore, the use of pre-insulated pipes has implied the simplification of the laying methods, employing cold laying instead of expansion facilities like compensators or U-bends, being more cost effective.² The PU foam layer needs to withstand the shear stresses without failure for the network lifetime to preserve its load bearing function. Knowledge on the ageing mechanisms of the PU foam is of great importance in order to ensure the pipe assembly performs as specified during its service life, as well as to assess if this service life could be extended.

The EN253:2019 standard¹ assumes that the failure of the PU bond and hence the service life is driven by

This is an open access article under the terms of the Creative Commons Attribution License, which permits use, distribution and reproduction in any medium, provided the original work is properly cited.

© 2020 The Authors. Fatigue & Fracture of Engineering Materials & Structures published by John Wiley & Sons Ltd

thermo-oxidative degradation of the PU, governed by an Arrhenius relationship. Studies on the accelerated ageing and thermal degradation of pre-insulated pipes^{3–6} show discrepancies between the results of the tests and the degradation process observed in the field. Cited explanations include that higher temperatures alter the degradation rather than accelerate it. Aspects like gas exchange with the environment are recently considered.

Previous projects and reports have dealt with the topic of thermal cycling and fatigue of DH systems.^{2,7} The studies however relate only to the steel service pipe, while the effects on the PU foam are insufficiently well known or studied.² The design guidelines for DH networks include fatigue check.⁸ However, again it relates to the steel pipe only, and stating the lack of knowledge, it assumes that fatigue does not occur on the foam within the limits of the permissible stresses. This highlights the research need for observing and understanding if and how cyclic loads could produce fatigue on the foam or facilitate debonding of the layers due to stresses at the interface.

2 | FATIGUE AND FRACTURE OF PU FOAM—STATE OF THE ART

The increasing use of PU sandwich composites as load bearing structures has triggered research on its fatigue and fracture behaviour in recent years. The most accepted mechanism for fatigue crack growth in cellular solids is the failure of a cell wall ahead of the crack tip after repeated flexure, causing a step-wise crack growth, one cell at a time.⁹ Empirical observations of crack propagation through cell walls and the adjacent struts confirm this.^{10,11} Huang and Lin¹² have proposed a model for fatigue crack growth rate consistent with this mechanism. They conclude that fatigue of cellular materials depends on cyclic stress intensity range, cell size, relative density and the fatigue parameters of the solid from which they are made. Zenkert et al.¹³ follow a different approach, assuming crack growth in closed cell polymeric foams to be continuous and not cell-size dependent. Their model relates crack propagation rate behaviour with their un-notched fatigue life. However, it is reported that crack propagation in foams is interrupted by crack bridging by cell edges,^{10,14} which differentiates crack propagation in foams from that in solids. In this regard, Olurin¹⁵ suggests that the fatigue crack growth rate in an aluminium alloy foam is controlled by the progressive degradation of crack bridging by fatigue failure of the cell edges behind the crack tip. In a previous work by the team, it was argued that the fatigue degradation mechanism is material ratcheting due to progressive strain accumulation, rather than cracking

events in the foam.¹⁶ This is in contrast with the report of Burman¹⁷ that fatigue crack nucleation appears over a large volume of the test specimen, later converging to a macroscopic crack. The governing mechanisms are therefore not yet fully understood.

Another followed approach is the experimental characterization of mechanical behaviour and the development of empirical failure criteria. Marsavina and coworkers have characterized the fracture of PU foams, comparing dynamic and static fracture toughness,¹⁸ the effects of density, anisotropy, loading speed and mix mode ratio,¹⁹ and Modes I and II fracture toughness for different types of specimens.²⁰ They have found that density exerts the main influence on the results, dynamic fracture toughness is higher than static, and increase in loading speed produces a decrease of Mode I but no effect on Mode II fracture toughness.

On fatigue tests of foam core sandwich structures under higher temperatures, Kanny et al.²¹ report that crosslinks provide mechanical stability of the PVC cores under temperature, extending their fatigue life, while an inverse behaviour is observed at room temperature.

The type of loading, constituent material properties and geometrical dimensions condition the initiation, propagation and interaction of failure modes.²² In a previous work, we have found that PU in pre-insulated pipes presents a much higher anisotropy in both the microstructure and the mechanical properties under compression than that previously reported for PU slabs, arising from the different geometry of the mould during the foaming process.²³ This, together with the different geometry of the sample, an annular pipe, and the effect of high temperature, highlights the need for specific evaluation of this element.

The focus of this work lies in observing and understanding if and how cyclic loads affect the shear strength (τ_{\max}), shear modulus (G), toughness (U) and failure behaviour of the PU foam in DH pipes sandwich assembly compared with unaged reference samples.

3 | MATERIALS AND METHODS

3.1 | Cyclic loading tests

Samples were machined out of commercial DN20 pipes with 28.5 mm insulation thickness and 6-m length (Logstor A/S, Denmark), following EN 253:2019.¹ All samples were produced with a length $L = 200$ mm and were individually accurately measured using a caliper and weighed prior to testing. The foam is cyclopentane-blown closed-cell PU with an average density of 76.2 kg/m³. Details on the microstructural

characterization have been presented in Doyle et al.²³ The ends of the pipe samples were not sealed and in direct contact with air. However, previous research from accelerated ageing of PU pre-insulated pipes under equivalent high ambient temperature have shown that changes in shear strength do not depend on the thermo-oxidation of PU at the temperatures under consideration²⁴ and therefore this should not have a relevant impact on the obtained results.

Three different cyclic loading trials were carried out, as summarized in Table 1.

3.1.1 | Trial T: Thermal cycles

For trial T, five specimens were subjected to thermal cycling inside a thermal chamber (Weiss WK1 340, Reiskirchen, Germany). Temperature was varied between 25°C and 100°C, which is the maximum operation temperature of the chamber and close to DH networks operation temperature. The number of cycles was set at 250, which is the number of cycles established for fatigue check for secondary effects for distribution lines according to AGFW e.V.⁸ Initial trials were conducted to measure the required time needed for the steel service pipe to reach thermal equilibrium at 100°C, which was

measured as 75 min. The heating and cooling ramp was established as 30 min, as it should not be as fast as to induce thermal shock, which would lead to a different type of stresses, and is the time length defined by EN 253:2019¹ to achieve the high temperature for axial shear strength at 140°C.

The specimens were allowed to freely expand and contract. Therefore, the stresses produced by these thermal cycles are due to the mismatch in coefficient of thermal expansion of the materials, which is higher for the PU foam than for the steel.

3.1.2 | Trial MT-wc: Thermal and mechanical cycles—Worst case conditions

Because the pipes under operating conditions do not freely expand but are subjected to axial shear stresses due to the soil friction forces, in this trial, axial shear stresses were mechanically induced in addition to the thermal cyclic loads described and applied in Trial T. For this, a specific test rig was designed in-house for the simultaneous testing of five samples inside of the thermal chamber. An axial force is exerted on the steel medium pipe by means of pneumatic valves (Festo AG, Esslingen am Neckar, Germany), while a ring at the base prevents movement of the casing, hence producing a shear stress along the foam. The electronic control of the mechanical cycling rig was coupled with a thermocouple placed in the middle specimen. This ensured that the maximum force was applied simultaneously to the maximum T° . A schematic of the test rig is presented in Figure 1.

For the selection of the applied force, a worst case scenario criterion was selected. Because EN 253:2019¹ establishes aged pipes should still withstand a shear stress of

TABLE 1 Parameters for the executed cyclic loading trials

Trial	T° interval (°C)	τ interval (MPa)	Number of cycles
T	25–100	0	250
MT-wc	25–100	0–0.12	250
MT-m	25–70	0–0.04	125

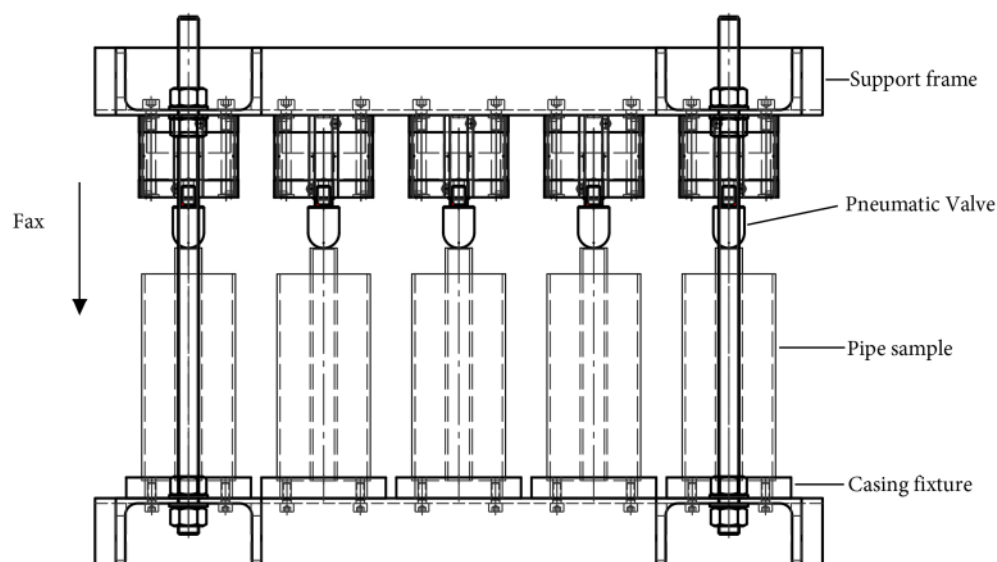


FIGURE 1 Test rig for mechanical cycling [Colour figure can be viewed at wileyonlinelibrary.com]

0.12 MPa at room temperature, this stress was selected, and the force to be applied is calculated as

$$F_{ax} = \tau \cdot L \cdot D_s \cdot \pi, \quad (1)$$

F_{ax} is the axial force

τ = shear stress

L = length of the pipe sample

D_s = diameter of the steel medium pipe.

This is a worst case scenario because

- The 0.12 MPa will be applied in the trial when the pipes are at 100°C and not at room temperature.
- According to the network design guidelines, the design shear stresses for operating conditions are 0.04 MPa.⁸

The number of cycles selected was again 250.

3.1.3 | Trial MT-m: Thermal and mechanical cycles—Mild conditions

In this trial, the mechanically applied shear stresses were set at 0.04 MPa. These stresses were applied in cycles from 0 to 0.04 MPa with the same frequency as in the previous trials. This value was selected as it is the acting shear stress under the network design point.⁸ The temperature was cycled between 25°C and 70°C, because buckling of the PE casing was experienced in trial MT-wc, as 100°C is too close to its heat deflecting temperature (Section 4). The number of cycles conducted was 125, representing half of the established number of cycles for fatigue check of DH pipes.

3.2 | Static tests

The test setup was chosen according to EN 253. The axial force was applied on the steel medium pipe until failure of the foam with a crosshead displacement controlled speed of 5 mm/min. The force was measured with a 20-kN load cell, accuracy class 0.5 (HBM, Darmstadt, Germany). Because the casing is fixed, the relative displacement between the steel medium pipe and the casing produces shear strain on the foam. The shear strain was calculated as

$$\gamma = \frac{u}{a}, \quad (2)$$

where u is the displacement of the steel medium pipe relative to the pipe casing and a is the thickness of the foam, equal to 28.5 mm.

The displacement was measured by three-dimensional (3-D) digital image correlation (DIC)²⁵ using an ARAMIS 5M adjustable stereo camera system (GOM mbH, Braunschweig, Germany) with a resolution of 2448 × 2051 pixels. The images were acquired at frequency of 1 Hz. Reference point markers were used to measure and track the 3D coordinates during the tests. Figure 2 presents a sketch of the test setup.

Five unaged samples were tested to obtain the reference values of strength, stiffness and toughness. For samples aged under cyclic loading, careful examination of possible damage or failure was undertaken and photographically documented prior to the execution of the static tests. Reweighing and remeasuring was undertaken. Seventy-two hours was allowed between the finalization of the cycles and the axial shear test to ensure stable conditions of the samples.

Additional static tests of unaged specimens were conducted under temperature, as to derive the acting stresses during the cyclic loading trials. For this, an environmental chamber (Weiss WK3-180/70/5-UKA, Reiskirchen, Germany) was placed around the universal testing machine. Samples were temperature soaked overnight to ensure stable conditions prior testing. Five specimens were tested at 70°C. Only one sample was tested at 100°C as it was decided to stop the tests after observing the buckling in the casing due to softening of the PE casing at that temperature.

Engineering stress–strain curves were derived from the obtained data. As per EN253, the shear stress is calculated from Equation 1.

The standard assumes that the maximum axial stresses are acting in the area continuous to the steel pipe. This is because it is the smallest area of the foam in the pipe section subjected to shear stresses. Our results show that indeed this is the area where the crack initiates (see Section 4). The shear strength is taken as the maximum value of the curve.

The G modulus is determined for each case from the slope of the initial linear segment of the curves.

The toughness (U) was calculated from the integral under the stress–strain curve until the strain upon failure is reached, at maximum value of τ of the curve

$$U = \int_0^{\gamma_f} \tau \cdot d\gamma, \quad (3)$$

where

γ is the shear strain

γ_f is the shear strain upon failure

τ is the shear stress.

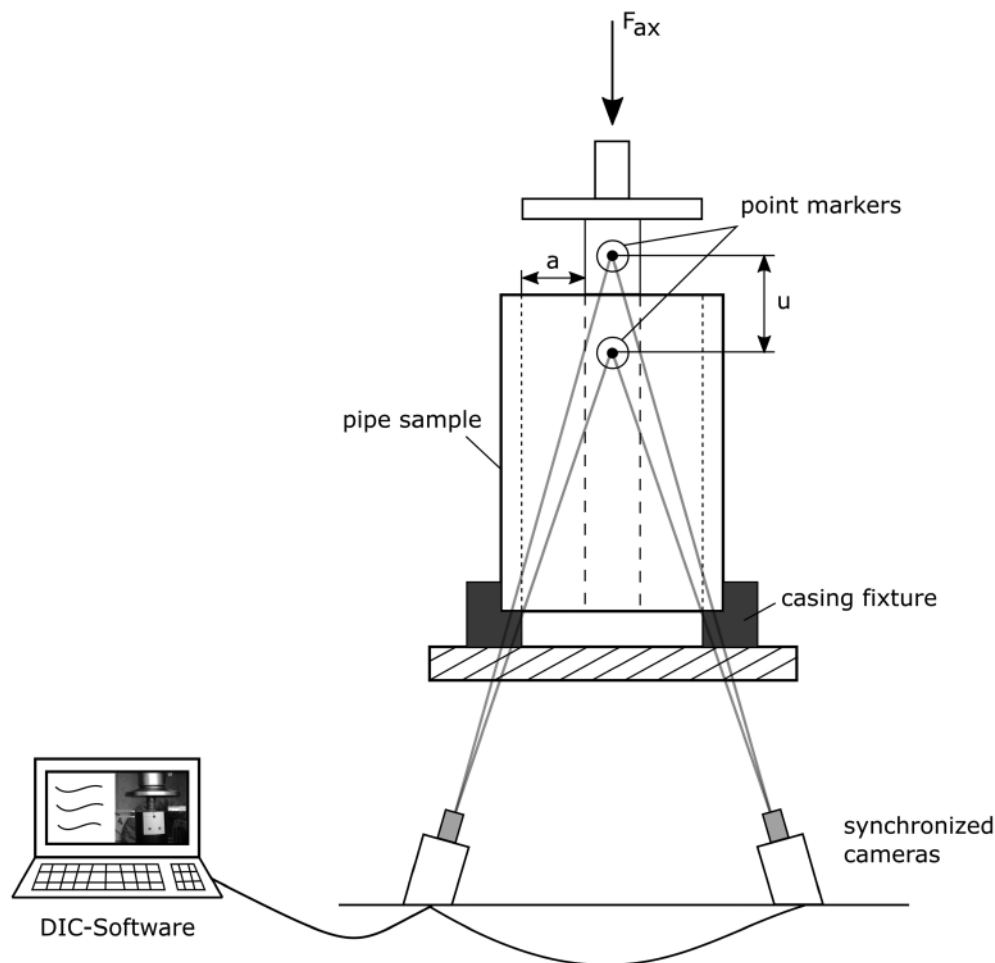


FIGURE 2 Schematic drawing of the static test setup. DIC, digital image correlation

3.3 | Evaluation of alterations in the chemical structure of the PU foam

Possible alterations in the chemical structure of the PU foam were evaluated through Fourier transform infrared spectroscopy (FTIR) in attenuated total reflection (ATR) mode^{3,26–29} using a Thermo Scientific Nicolet is 10 FTIR spectrometer with a diamond ATR Smart Orbit accessory (Dreieich, Germany). Infrared spectra were collected in transmission mode from 32 co-added scans and 6 cm^{-1} spectral resolution and converted to absorption as to allow linear correspondence between concentration and peak area. Spectra were baseline corrected, and the integrated absorbance for selected peaks were normalized using the C=C stretching vibration in the aromatic ring at 1595 cm^{-1} to correct for sample thickness differences. For each evaluated pipe, five foam samples were analysed, taken along the axial direction of the pipe, from the area in the vicinity of the steel medium pipe. Because the foam from unaged pipes presents a higher variability in their mechanical behaviour, foam from three unaged pipes was analysed, and one from each ageing trial. Assignments for many PU absorption bands can be found

in several publications.^{3,27,30} The focus was placed on observing potential post curing through changes on the concentration of non-reacted isocyanates (2270 cm^{-1}) and urethane linkages (1714 cm^{-1}), thermo-oxidative degradation and chain scissoring through changes in urethane linkages (1714 cm^{-1}) and CH_2 groups (peaks between 2975 and 2872 cm^{-1}) and changes in the strength of H bonds through the stretching vibration of the N-H groups (3302 cm^{-1}), and shift between H-bonded urea (1640 cm^{-1}) and monodentate urea (1650–1680 cm^{-1}).

3.4 | Documentation of crack propagation

In order to gain knowledge on the fracture and failure of the pre-insulated pipes, the resulting cracks from the static tests were photographically documented with a digital camera. The tested pipes were axially cut as to observe the crack propagation through interior of the foam. Prior to the cutting, a coloured epoxy resin was introduced through the cracks as to highlight them and evaluate their interconnections through the length of the pipe.

4 | RESULTS

4.1 | Effects of cyclic loads on the mechanical behaviour of the pre-insulated pipes

After the finalization of the programmed load cycles no weight change detected in any of the tested specimens, nor damage or geometry change for specimens from trials T or MT-m. A yellowing of the specimens after ageing was observed for the samples aged with 250 cycles (T and MT-wc), which is as a sign for thermo-oxidative degradation.³ After later observation of the fractured pipes, it could be seen that this phenomenon was only superficial.

For the MT-wc trial, 24 of the 250 cycles were conducted with a constant stress of 0.12 MPa due to a malfunction of the control system. In this case, all five specimens exhibited compression and buckling of the casing at the bottom of the samples, as well as failure of the foam close to the steel interface, as can be seen in Figure 3. This caused a length reduction of the casing from 200 to approximately 196 mm. This can be related to the vicinity of the 100°C test T° to the melting T° of high-density PE (HDPE), which is in the range 118°C–146°C depending on molecular weight and crystallization conditions.³¹ Because the cycles were load controlled, we

do not know in which cycle the failure occurred. However, from the static test performed on an unaged sample at 100°C (see Section 3.4), the buckling occurred at 0.34 MPa, which is higher than the applied 0.12 MPa during the cyclic loading test. The failure at this load is therefore a consequence of the cyclic loading.

Figure 4 shows the obtained engineering stress–strain curve obtained through Trials T (A), MT-wc (B) and MT-m (C). Curves for the unaged samples tested at room conditions are added in all plots for reference. For the MT-wc trial, the damaged section of one of the specimens was removed before testing as to assess the impact of the pre-existing failure on the obtained results. The obtained max shear strength (τ_{max}), stiffness (G) and toughness (U) are presented in Table 2 and Figure 5.

4.2 | Effects of temperature on the mechanical behaviour of the pre-insulated pipes

The obtained stress–strain curves for unaged samples tested at different temperatures are shown in Figure 6, and obtained values for strength, stiffness and toughness presented in Table 3.

FIGURE 3 Buckling and compression of the casing (A) and failure of the foam at the foam–steel interface (B) after MT-wc trial [Colour figure can be viewed at wileyonlinelibrary.com]

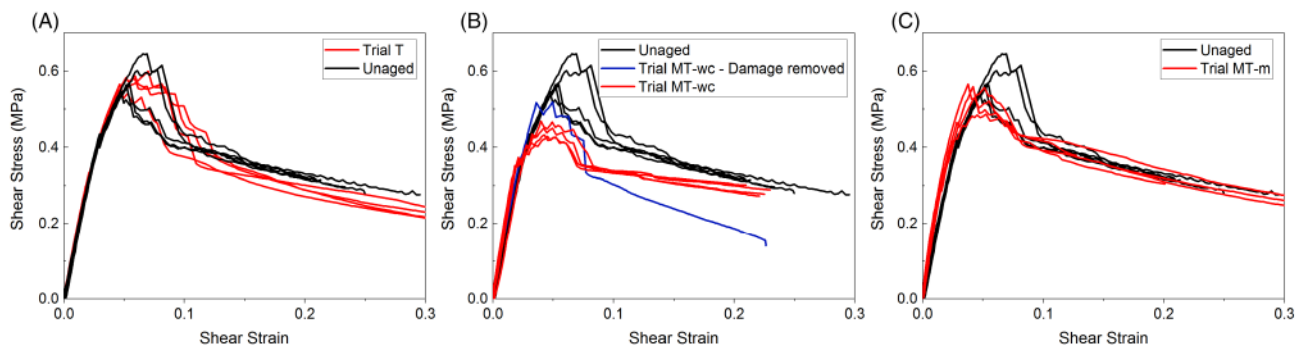
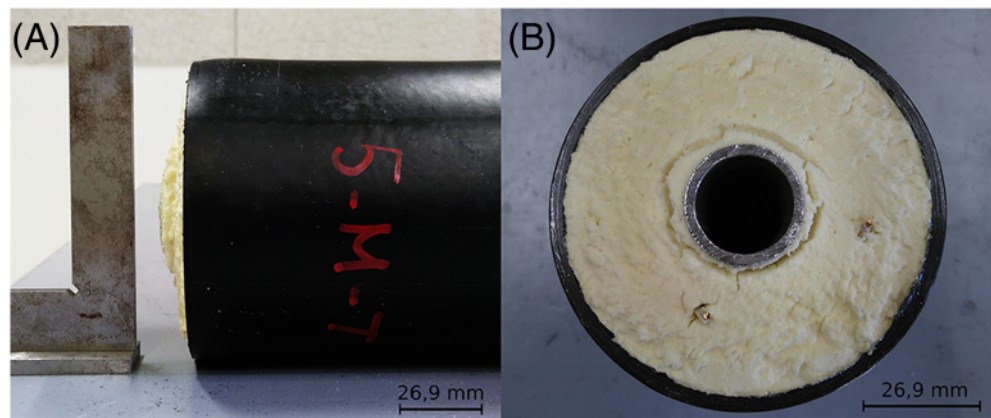


FIGURE 4 Stress–strain curves for static tests, unaged and after Trails T (A), MT-wc (B) and MT-m (C) [Colour figure can be viewed at wileyonlinelibrary.com]

TABLE 2 Results from static tests for different cycling trials

Cycling trials	τ_{max} (MPa)	G (MPa)	U (MJ/m ³)	γ_f
Unaged	0.58 ± 0.04^a	16.55 ± 0.51^a	0.019 ± 0.003^a	0.081 ± 0.063^a
MT-wc	0.45 ± 0.02^a	17.71 ± 2.34	0.013 ± 0.003^a	0.046 ± 0.003^a
MT-wc (damage removed)	0.52	16.52	0.010	0.035
T	0.58 ± 0.01^a	16.80 ± 0.51^a	0.022 ± 0.005^a	0.058 ± 0.0097^a
MT-m	0.54 ± 0.01^a	20.44 ± 0.77^a	0.015 ± 0.002^a	0.043 ± 0.0062^a

^aStandard deviation.

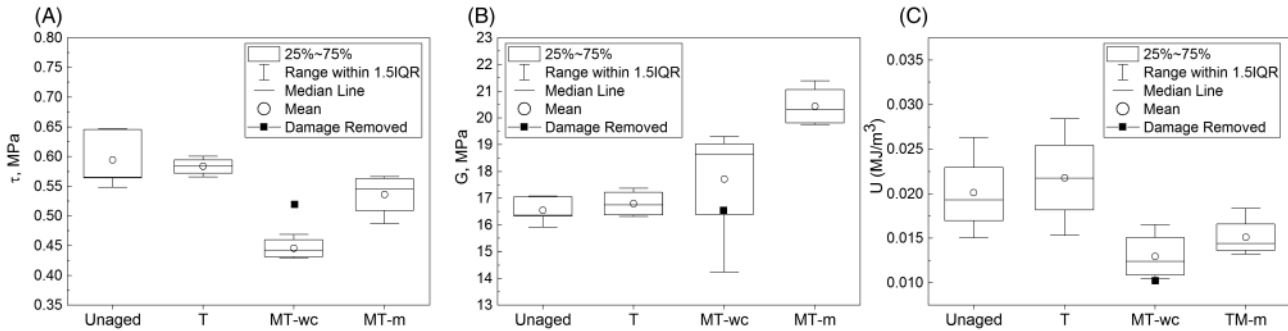


FIGURE 5 Obtained shear strength (A), stiffness (B) and toughness (C) for the conducted trials

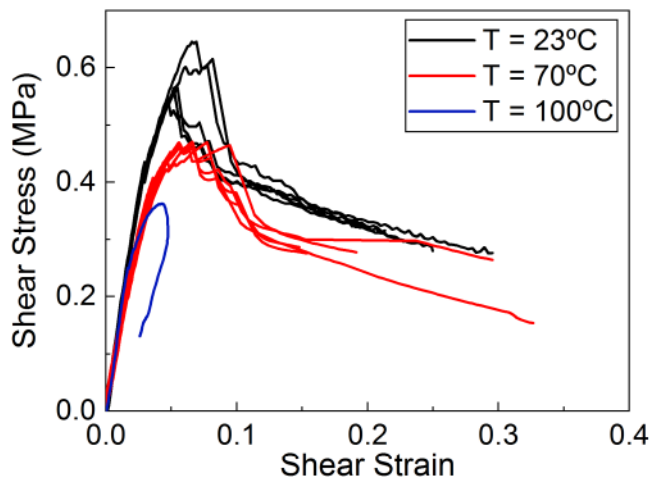


FIGURE 6 Stress-strain curve of unaged samples under different temperatures [Colour figure can be viewed at wileyonlinelibrary.com]

As previously indicated, for the test at 100°C, only one sample was tested. Due to the buckling, the strain is reduced after reaching a maximum, as the casing is no longer holding the applied load. However, through careful observation of the obtained stress-strain curve and the test digital images, valuable information towards the understanding of the failure of the specimens from trial MT-wc (see Section 3.1). While the maximum is reached at 0.36 MPa stress and 0.043 strain, the compression of the casing starts practically from the beginning of the test, although buckling is only evident starting at a loading of approximately 0.34 MPa. A first peak is observed at 0.25 MPa in the stress-strain curve, which could be the offset on which the failure of the foam and the buckling of the casing started. The buckling failure in the static test occurred at a higher stress than the 0.12 MPa applied in the cyclic loading, which is the point taken as the end

TABLE 3 Results from static tests conducted at different temperatures

T (°C)	τ_{max} (MPa)	G (MPa)	U (MJ/m ³)	γ_f
23	0.58 ± 0.04^a	16.55 ± 0.51^a	0.019 ± 0.003^a	0.081 ± 0.063^a
70	0.46 ± 0.003^a	13.42 ± 1.43^a	0.020 ± 0.004^a	0.063 ± 0.008^a
100	0.36	16.34	—	0.043

^aStandard deviation.

of the linear elastic region, showing that the failure at this stress was due to the effects of the cyclic loads.

As it can be seen, the shear strength is reduced by 20% and the modulus is reduced by 18% when testing at 70°C compared with 23°C. From these tests, we can derive that the acting strain during the cyclic loading tests was 0.008 for trial MT-wc and between 0.001 and 0.003 for trial MT-m.

4.3 | Evaluation of alterations in the chemical structure of the PU foam

PU presents a segmented structure, consisting of a soft segment originating from the polyol chain, and a hard segment, mainly composed of aromatic rings bonded together through urea linkages. The urethane bond chemically links both segments covalently. When the diisocyanate is in excess, further chemical cross linking can occur through the creation of allophanate linkages. The hard segments are strongly hydrogen bonded, which act as physical crosslinks²⁶ and are reported to have a significant impact on the PU's physical behaviour, increasing its mechanical properties,^{32,33} and also, the inhomogeneity of the material.²⁶ A degradation of the links, chemical and/or physical, would lead to a degradation in the PU foam's mechanical properties.

A typical spectrum obtained for an unaged sample with the identified peaks is shown in Figure 7.

The obtained normalized integrated absorbance for the selected peaks can be found in Figure 8.

Unreacted isocyanates were not detected in the obtained spectra. An increase in peak 1712 cm^{-1} would imply further curing of the PU from its unreacted components, while its decrease would imply scissoring of the chain. Thermo-oxidative degradation is reported to occur mainly in the soft segment³ and a decrease of the concentration of C–H links through the band at 2975–2872 cm^{-1} (evaluated through the peaks at 2928 and 2868 cm^{-1}) would be a sign of this. A decrease in the N–H stretch band at 3305 cm^{-1} and a shift from the bidentate urea at 1640 cm^{-1} to monodentate urea at 1650–1680 cm^{-1} would be a sign of weakening of the H bonds. The bidentate urea peak was not visible in the obtained spectra. Peak deconvolution was not attempted.

As it can be seen, the differences in the normalized absorbance for the selected peaks after cyclic loading are within the variability found in unaged samples. From this analysis, we can conclude that the applied cyclic loading did not produce changes in the molecular structure of the polymer matrix.

4.4 | Crack propagation

After sectioning the tested pipes, it was seen that the same crack pattern occurred consistently in all specimens, independently of aged or unaged. Seven to nine cracks appear through the axial length of the pipe, with a constant distance of 2–2.5 cm between them. They span from the area close to the foam–steel interface to approximately 2 cm away from the PE casing, in an

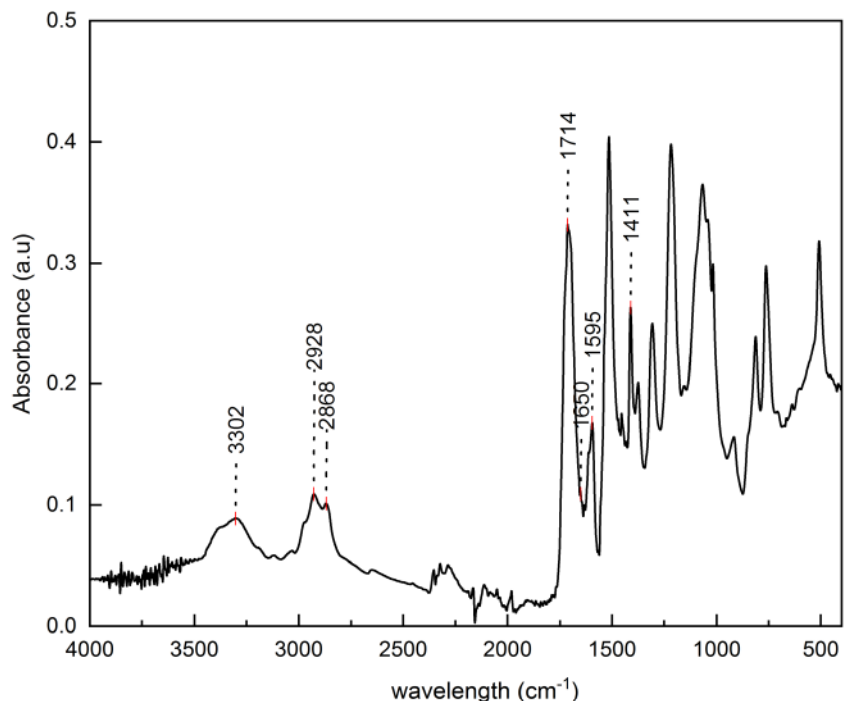


FIGURE 7 Obtained Fourier transform infrared spectroscopy (FTIR) for the foam of an unaged pipe [Colour figure can be viewed at wileyonlinelibrary.com]

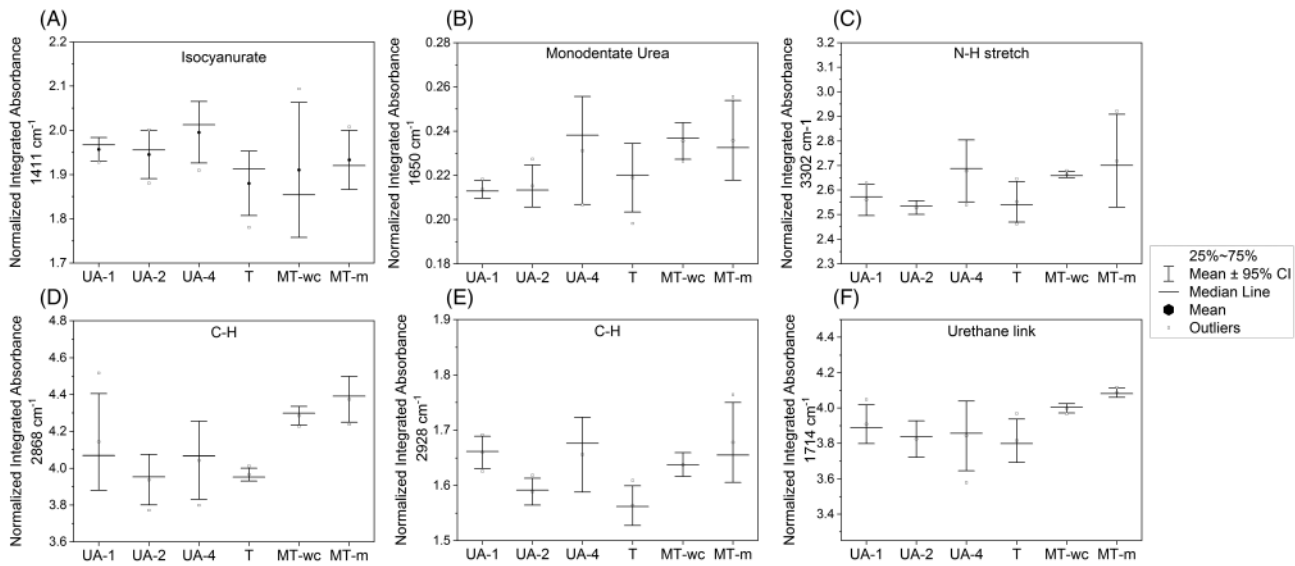


FIGURE 8 Normalized integrated absorbance for selected peaks (A–F), for unaged (UA) pipes, T, MT-wc and MT-m cycled pipes. CI, confidence interval

approximately 45° angle with the horizontal. Only the bottom crack reaches the PE casing, which could be the result of the stress concentrations by the test fixture on the casing. From this pattern, we can derive that the cracks initiate in Mode II fracture close to the steel interface, which is the area where the shear stresses are maximum, and then kink and propagate in Mode I fracture.

For the MT-wc specimens (Figure 9A), different colours were used for the initial failure near the foam–steel interface due to the cyclic loads (red) and that close to the foam-casing due to the static test (blue). It could be seen that the initial failure propagated through the foam–steel interface approximately 1/3 or the pipe length, interconnecting the first and third cracks.

As for the fracture type, from the evaluation of the specimens after shear tests, it can be observed that for the 18 specimens tested at room temperature, aged and unaged, cohesive fracture occurred in the foam, except for one case where both failure of the adhesion of the PU-steel bond and cohesive fracture of the foam occurred. For the specimens tested at 70°C Figure 9B and C), both adhesive and cohesive failure occurred in three out of five specimens. This could be easily observed as the coloured epoxy resin introduced through the cracks at the bottom of the specimens flowed until exiting at the steel–foam interface and colouring all cracks, showing they are interconnected, while for the case of specimens sheared at room

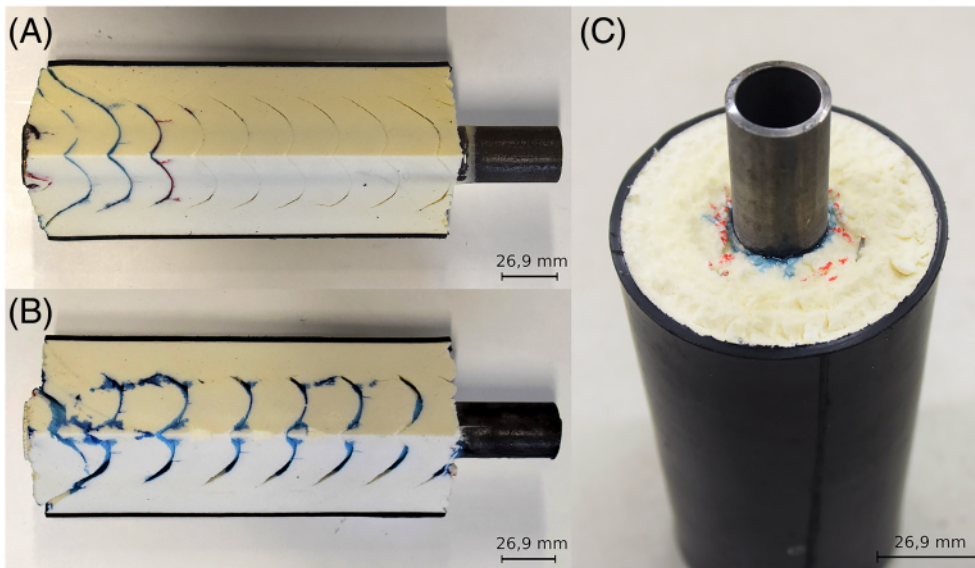


FIGURE 9 (A) Specimen tested at room temperature (MT-wc), (B) specimen tested at 70°C where the coloured resin flowed through the foam–steel interphase along the pipe, (C) detail of the foam–steel interface for the specimen tested at 70°C. The coloured resin proves loss of adhesion between them [Colour figure can be viewed at wileyonlinelibrary.com]

temperature, the colour only flowed through the first layers of cracks (see Figure 9).

5 | DISCUSSION

The main objective of this study is the evaluation of the impact of cyclic loads on the mechanical properties of the pre-insulated pipes. From Figure 5, we can observe that the combination of cyclic mechanical and thermal loads has a stronger effect on the mechanical properties of the pre-insulated pipes than the thermal loads on their own. Because the samples of the T series are under free expansion conditions, the caused strain is limited to the mismatch of thermal expansion between the material layers. From the obtained values of strength and stiffness, we can conclude that these strains are not enough to deteriorate the structure within the number of cycles under consideration. The main effect of the temperature loads is a homogenization of the behaviour between specimens, reducing the standard deviation of the measured strength values while maintaining the average values similar to the unaged control series. Foam-filled composites produced in batches for structural applications in the building sector present a higher variability in material properties than those manufactured in bulk and under tightly controlled curing conditions for applications such as shipping and aerospace.^{34,35} Therefore, the temperature could produce a post-curing effect on the PU, leading to a higher homogeneity between specimens. The post-curing would increase the number of links in the polymer matrix, which is consistent with the slight increase in toughness observed (Figure 5C), as more energy is required to fracture a larger number of links. Previous authors have reported an increase in strength^{3,6} and stiffness³⁵ of PU foam after an initial thermal ageing and related it to post-curing of the PU. However, this was not confirmed by our FTIR analysis (see Figure 8F).

A degradation of the strength and toughness of the pre-insulated pipes due to the combined thermal and mechanical loads can be observed from Figure 5A,C. The degradation is more severe for the MT-wc cycles, with an average 24% loss of strength versus 8.5% loss for the cycles under milder conditions. If we consider the strength obtained for the sample tested after removal of the damaged section, the strength reduction for the MT-wc trial is of approximately 11%. While this is the result of one sample only, it is very likely that test setup fixture caused stress concentration on the lower section of the pipes, leading to premature failure. It was observed during the execution of the tests that the fitting of the pipe in the fixture was tight, as the casing buckling had increased the sample diameter in that area. Influence of setup-

induced stress concentrations on results in shear tests is often encountered and reported.^{36,37}

From Figure 6B, we can observe a reduction of the experimental scatter in the G modulus with similar mean values between the control specimens and the T cycled specimens and an increase in the modulus for the thermal and mechanically cycled samples. This indicates that the mechanical cycles have a strain hardening effect on the foam. This would be caused by the orientation of the PU segments during extension,³⁸ facilitated as the higher temperature increases the mobility of the polymer chains. Our results show a higher increase of the stiffness for the MT-m trial than the MT-wc, which was subjected to higher stress and number of cycles. Previous authors have reported that the hardening effect is confined to the first several cycles.³⁸ This could imply that the initial cycles produce a hardening effect, as obtained in trial MT-m, and that the additional cycles conducted in trial MT-wc would produce a degradation of the stiffness from the hardened state.

As for the effects of temperature on the static tests, the mechanical properties of the foam decrease with increasing temperature, as expected. As can be seen from Tables 2 and 3, the effect of temperature on the mechanical behaviour of the foam is stronger than the effect of the ageing itself. The glass transition temperature (T_g) of PU is set around 200°C–250°C.⁹ Below this T_g , the polymer is in the glassy regime, being the modulus directly linked with the Van-der-Waals intermolecular bonds, which are influenced by T_g , causing the stiffness to decrease with increasing temperature.²¹ As mentioned earlier, a source of strength in the PU foam are the H bonds in the hard segment. Previous studies have shown that these H bonds in PU foam are disrupted at temperatures starting around 40°C^{28,39} and this disruption is the most probable cause of loss of strength for our tests under temperature. These H bonds would reform as the temperature is brought back to ambient temperature. Permanent bond disruption could take place if an H bond is replaced by a water molecule, as proposed by Herrington and Klarfeld.⁴⁰ These water to water H bonds could break upon compression of the foam, allowing for chain slippage. França de Sá et al.²⁷ propose that the elimination of some bonded interactions would enable the penetration of further water molecules as well as the interaction of oxidation products into the free space between the hard segment chains, leading to the formation of new H-bonding interactions between these compounds and the urea group. Because the relative humidity inside both environmental chambers used was close to zero, permanent H-bond disruption or replacement would be unlikely, as confirmed through our FTIR analysis of the post-cycled samples (see Figure 8B).

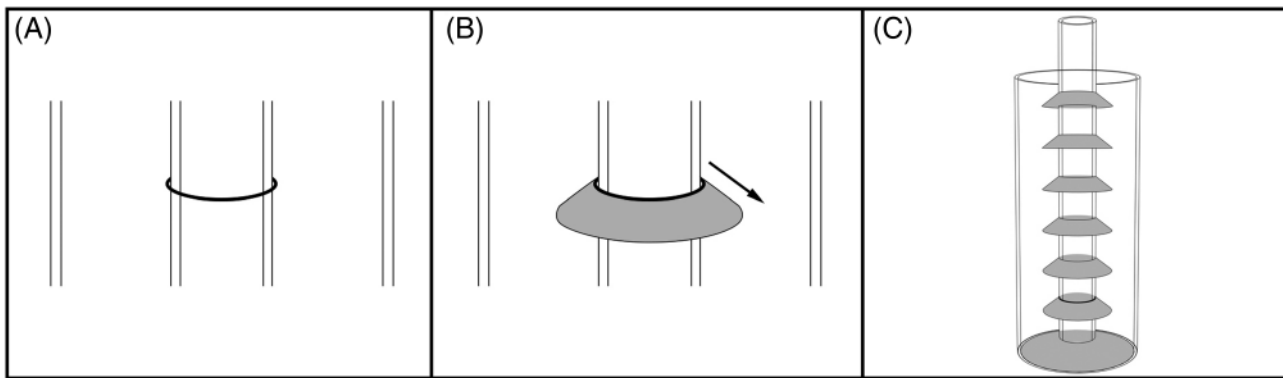


FIGURE 10 (A–C) Crack initiation and propagation in the polyurethane (PU) foam. Shaded areas represent crack planes

Thermal oxidation PU was not found to have occurred during the applied cycles, consistent with the findings of previous authors given the maximum applied temperature of 100°C.^{3,24,41} This means that the loss of mechanical properties as a consequence of the applied cyclic loads is not due to molecular changes on the polymer matrix, but could be related to other phenomenon as stress relaxation or fatigue.

As for crack propagation through the foam, propagation in Mode I is observed. Previous experimental studies indicate that this is the most common crack propagation mode in foam sandwich structures.^{37,42} The consistent distance between cracks indicate that the foam experiences strain localizations in the axial direction, displaced by approximately 2-cm intervals, which are the main driver for the crack nucleation. Pre-existing voids or other defects would produce cracks located randomly. This provides interesting information for the failure evaluation of the piping networks. A schematic drawing of the crack initiation, propagation and resulting fracture pattern is presented in Figure 10.

Concerning the fracture type, previous research on the cohesive laws between PU and galvanized steel⁴³ concluded that the fracture energy of the interface for Mode I tests appeared similar than that of the PU foam, with similar energy release rates for both interfacial failure and fracture of the foam cells adjacent to the interface, suggesting failure of the foam. But the adhesive bond strength at the interface also decreases with the increase in temperature. Fatigue studies on PU sandwich structures⁴⁴ report that debonding occurs when testing at higher frequencies due to increase in temperature at the mating surfaces. This suggests that, when conducting the shear tests at elevated temperatures, the strength of the adhesive bond between the foam and the steel is reduced, facilitating failure at the interface, while at room temperature, the predominant failure mechanism is cohesive fracture of the foam.

6 | CONCLUSIONS AND OUTLOOK

The main conclusions of our work are as follows:

- The combined cyclic thermal and mechanical loads evaluated in our trials have an effect on the PU foam, reducing its shear strength and increasing its stiffness. Despite this reduction, all the aged samples of the three executed trials would comply with the minimum shear strength requirement of EN253.
- Temperature has an important influence on the mechanical behaviour of the PU foam. The change in mechanical properties at the operating conditions of DH networks for the PU foam is significantly higher than for steel. Therefore, calculations for the steel pipe cannot be assumed to be valid for the sandwich composite.
- Crack initiation and propagation along the pipe samples follow a very consistent pattern between samples, with cracks initiating in Mode II and propagating in Mode I. The consistent axial displacement of approximately 2 cm from each other suggest the formation of strain localizations.
- At room temperature, cohesive fracture of the foam is obtained, while at higher temperatures, both adhesive failure at the foam–steel interface and cohesive fracture of the foam are found.

The presented work is limited to the investigated pipe dimensions representing household connections. The evaluation of the transferability of the results to distribution and main DH pipelines with larger dimensions requires further investigation.

ACKNOWLEDGEMENTS

The authors would like to express their gratitude to Logstor A/S (Løgstør, Denmark) and in particular Peter Jorsal and Tobias Langer for providing the district

heating pipes and discussions about the foam formulation. Assistance by Marcus Illguth for the design of the mechanical cyclic test rig, Jens Ohlendieck for the execution of the static tests, and Erik Borrs for the acquisition of the FTIR spectra are gracefully acknowledged.

This research was self-funded by the HafenCity University. Open access funding enabled and organized by Projekt DEAL.

CONFLICT OF INTEREST

The authors declare to have no conflict of interest.

AUTHOR CONTRIBUTION

I. W. was responsible for the study conceptualization and supervision of the research project. L. D. was responsible for the design of experiments, data collection and analysis and chiefly responsible for preparing the manuscript. Both authors contributed with the critical discussion of results and editing of the manuscript.

NOMENCLATURE

a	foam thickness
D_s	diameter of steel medium pipe
F_{ax}	axial force
G	shear modulus
L	pipe sample length
T_g	glass transition temperature
U	toughness
u	displacement
γ	shear strain
γ_f	shear strain at failure
τ	shear stress
τ_{max}	shear strength

ORCID

Lucia Doyle  <https://orcid.org/0000-0001-8697-8621>

Ingo Weidlich  <https://orcid.org/0000-0003-2653-0133>

REFERENCES

- EN 253:2019. District heating pipes. Bonded single pipe systems for directly buried hot water networks. Factory made pipe assembly of steel service pipe, polyurethane thermal insulation and a casing of polyethylene.
- Christensen. Fatigue analysis of district heating systems. *Netherlands Agency for Energy and the Environment* 1999
- Yarahmadi N, Vega A, Jakubowicz I. Accelerated ageing and degradation characteristics of rigid polyurethane foam. *Polym Degrad Stab.* 2017;138:192-200.
- Leuteritz A, Döring K-D, Lampke T, Kuehnert I. Accelerated ageing of plastic jacket pipes for district heating. *Polym Test.* 2016;51:142-147.
- Vega A, Yarahmadi N, Jakubowicz I. Optimal conditions for accelerated thermal ageing of district heating pipes. *Energy Procedia.* 2018;149:79-83.
- Vega A, Yarahmadi N, Jakubowicz I. Determination of the long-term performance of district heating pipes through accelerated ageing. *Polym Degrad Stab.* 2018;153:15-22.
- Randlov P, Hansen KE, Penderos M. Temperature variations in preinsulated DH pipes low cycle fatigue. <http://www.ieadhc.org/the-research/annexes/1993-1996-annex-iv/annex-iv-project-06.html>
- AGFW e.V, ed. Installation and calculations of preinsulated bonded pipes for district heating networks. *Static design; basics of stress analysis*
- Gibson LJ, Ashby MF. *Cellular Solids.* Cambridge: Cambridge University Press; 1997.
- Cotgreave T, Shortall JB. Failure mechanisms in fibre reinforced rigid polyurethane foam. *J Cell Plast.* 1977;13(4): 240-244.
- Ridha M. Mechanical and Failure Properties of rigid Polyurethane Foam Under Tension. *PhD Dissertation*, National University of Singapore, 2007
- Huang JS, Lin JY. Fatigue of cellular materials. *Acta Mater.* 1996;44(1):289-296.
- Zenkert D, Shipsha A, Burman M. Fatigue of closed cell foams. *J Sandw Struct Mater.* 2006;8(6):517-538.
- McCullough KYG, Fleck NA, Ashby MF. Toughness of aluminium alloy foams. *Acta Mater.* 1999;47(8):2331-2343.
- Olurin O. Fatigue crack propagation in aluminium alloy foams. *Int J Fatigue.* 2001;23(5):375-382.
- McCullough KYG, Fleck NA. The stress-life fatigue behaviour of aluminium alloy foams. *Fatigue Fract Eng Mater Struct.* 2000; 23(3):199-208. <https://doi.org/10.1046/j.1460-2695.2000.00261.x>
- Burman M. Fatigue Crack Initiation and Propagation in Sandwich Structures. *PhD. Dissertation*, Royal Institute of Technology, Sweden, 1998
- Marsavina L, Linul E, Voiconi T, Sadowski T. A comparison between dynamic and static fracture toughness of polyurethane foams. *Polym Test.* 2013;32(4):673-680.
- Marsavina L, Constantinescu DM, Linul E, Apostol DA, Voiconi T, Sadowski T. Refinements on fracture toughness of PUR foams. *Eng Fract Mech.* 2014;129:54-66.
- Marsavina L, Constantinescu DM, Linul E, Voiconi T, Apostol DA. Shear and mode II fracture of PUR foams. *Eng Fail Anal.* 2015;58:465-476.
- Kanny K, Mahfuz H, Thomas T, Jeelani S. Temperature effects on the fatigue behavior of foam core sandwich structures. *Polym Polym Compos.* 2004;12(7):551-559.
- Linul E, Masavina L. Assessment of sandwich beams with rigid polyurethane foam core using failure-mode maps. *Proceedings of the Romanian Academy*, 2015
- Doyle L, Weidlich I, Illguth M. Anisotropy in Polyurethane Pre-Insulated Pipes. *Polymers.* 2019;11:2074. <https://doi.org/10.3390/polym11122074>
- Yarahmadi N, Sällström JH. Improved maintenance strategies for district heating pipe-lines. *IEA-DHC final report, Annex X*, Stockholm, Sweden, 2014
- Peters WH, Ranson WF. Digital Imaging Techniques In Experimental Stress Analysis. *Opt Eng.* 1982;21(3):427-431. <https://doi.org/10.1117/12.7972925>

26. Kontou E, Spathis G, Niaounakis M, Kefalas V. Physical and chemical cross-linking effects in polyurethane elastomers. *Colloid Polym Sci*. 1990;268(7):636-644.
27. França de Sá S, Ferreira JL, Pombo Cardoso I, Macedo R, Ramos AM. Shedding new light on polyurethane degradation: assessing foams condition in design objects. *Polym Degrad Stab*. 2017;144:354-365.
28. Senich GA, MacKnight WJ. Fourier transform infrared thermal analysis of a segmented polyurethane. *Macromolecules*. 1980;13(1):106-110.
29. Cole KC, van Gheluwe P, Hébrard MJ, Leroux J. Flexible polyurethane foam. I. FTIR analysis of residual isocyanate. *J Appl Polym Sci*. 1987;34:395-407.
30. Hepburn C. *Polyurethane Elastomers*. Dordrecht: Springer Netherlands; 2000.
31. Mark JE (Ed). *Polymer Data Handbook*. New York: Oxford University Press; 1999.
32. Petrović ZS, Ilavský M, Dusek K, Vidaković M, Javni I, Banjanin B. The effect of crosslinking on properties of polyurethane elastomers. *J Appl Polym Sci*. 1991;42:391-398.
33. Smith TL. Strength of elastomers, a perspective. *Polym Eng Sci*. 1977;17(3):129-143.
34. Banerjee B, Kraus B, Das R. Characterization of an anisotropic low-density closed-cell polyurethane foam: Unpublished, 2015
35. Tuwair H, Volz J, ElGawady M, Mohamed M, Chandrashekhara K, Birman V. Behavior of GFRP bridge deck panels infilled with polyurethane foam under various environmental exposure. *Structure*. 2016;5:141-151.
36. Gdoutos EE, Daniel IM, Wang K-A. Failure of cellular foams under multiaxial loading. *Compos A: Appl Sci Manuf*. 2002;33(2):163-176.
37. Gibson RF. A mechanics of materials/fracture mechanics analysis of core shear failure in foam core composite sandwich beams. *J Sandw Struct Mater*. 2011;13(1):83-95.
38. Kim BK, Lee SY, Xu M. Polyurethanes having shape memory effects. *Polymer*. 1996;37(26):5781-5793.
39. Teo L-S, Chen C-Y, Kuo J-F. Fourier transform infrared spectroscopy study on effects of temperature on hydrogen bonding in amine-containing polyurethanes and poly (urethane-urea)s. *Macromolecules*. 1997;30(6):1793-1799.
40. Herrington RM, Klarfeld DL. Humid aged compression set phenomena in water blown Hr molded foams. *J Cell Plast*. 1984;20(1):58-63.
41. Yarahmadi N, Vega A, Jakubowicz I. Determination of essential parameters influencing service life time of polyurethane insulation in district heating pipes. *Energy Procedia*. 2017;116:320-323.
42. Carlsson L, Matteson R, Aviles F, Loup D. Crack path in foam cored DCB sandwich fracture specimens. *Compos Sci Technol*. 2005;65(15-16):2612-2621.
43. Kraus B, Das R, Banerjee B. Characterization of Cohesive Laws for Foam-Metal Interfaces. *Int J Appl Mech*. 2014;6:1450072-1-1450072-31. <https://doi.org/10.1142/s1758825114500720>
44. Sharma SC, Murthy HNN, Krishna M. Interfacial studies in fatigue behavior of polyurethane Sandwich structures. *J Reinf Plast Comp*. 2004;23(8):893-903.

How to cite this article: Doyle L, Weidlich I. Effects of thermal and mechanical cyclic loads on polyurethane pre-insulated pipes. *Fatigue Fract Eng Mater Struct*. 2021;44:156-168. <https://doi.org/10.1111/ffe.13347>